fibers

MDPI

Article

Electrospun Carbon Fibers from Green Solvent-Fractionated Kraft Lignin

Marta Goliszek-Chabros [1,*] and Omid Hosseinaei [2,*]

[1] Analytical Laboratory, Institute of Chemical Science, Faculty of Chemistry, Maria Curie-Skłodowska University, M. Curie-Skłodowska Sq. 3, 20-031 Lublin, Poland
[2] RISE Research Institutes of Sweden, Drottning Kristinas väg 61, 114 28 Stockholm, Sweden
* Correspondence: marta.goliszek-chabros@mail.umcs.pl (M.G.-C.); omid.hosseinaei@ri.se (O.H.)

Abstract

High production costs and sustainability issues are the main factors limiting the widespread application of carbon fibers in various industrial sectors. Lignin, a by-product from the paper and pulping industry, due to its high carbon content of up to 60%, can be considered a potential replacement for polyacrylonitrile in carbon fiber production. The production of lignins with distinct molecular weight distributions as well as group functionalities is essential to enhance high-value applications of lignin. In this study, we present a simple, green solvent-based fractionation method for LignoBoost softwood kraft lignin to obtain a lignin fraction with tailored physicochemical properties for electrospun carbon fiber production without polymeric spinning additives. Sequential solvent extraction was used to produce two fractions with distinct molecular weights: low-molecular-weight softwood kraft lignin (LMW-SKL) and high-molecular-weight softwood kraft lignin (HMW-SKL). The lignin fractions were characterized using size exclusion chromatography (SEC) for the molar mass distribution. The thermal properties of lignins were studied using thermogravimetry (TGA) and differential scanning calorimetry (DSC). Hydroxyl group content was quantified using quantitative ^{31}P NMR spectroscopy. We successfully demonstrated the electrospinning of a high-molecular-weight lignin fraction—obtained in high yield from the fractionation process—without the use of any additives, followed by thermal conversion to produce electrospun carbon fibers. The presented results contribute to the valorization of lignin as well as to the development of green and sustainable technologies.

Keywords: lignin; solvent fractionation; electrospinning; electrospun carbon fibers

check for updates

Academic Editor: Ramiro Rafael Ruiz Rosas

Received: 13 October 2025
Revised: 14 November 2025
Accepted: 2 December 2025
Published: 4 December 2025

Citation: Goliszek-Chabros, M.; Hosseinaei, O. Electrospun Carbon Fibers from Green Solvent-Fractionated Kraft Lignin. *Fibers* **2025**, *13*, 162. https://doi.org/10.3390/fib13120162

Copyright: © 2025 by the authors. Licensee MDPI, Basel, Switzerland. This article is an open access article distributed under the terms and conditions of the Creative Commons Attribution (CC BY) license (https://creativecommons.org/licenses/by/4.0/).

1. Introduction

Lignin is the second most abundant natural polymer on Earth after cellulose. It accounts for around 30% of the organic carbon that exists in the biosphere, and it is the main biorenewable source of aromatic structures. Lignin is formed by three precursor substances, namely *p*-coumaryl alcohol, coniferyl alcohol, and sinapyl alcohol, corresponding to the *p*-hydroxyphenyl (H), guaiacyl (G), and syringyl (S) structural units, respectively. The role of lignin in the plant cell wall is to provide supportive and impermeability functions in the vascular tissue, as well as protection against pathogens. The pulp and paper industry produces approximately 70 million tons of lignin annually. Unfortunately, only about 2% of the lignin is utilized effectively. Most of it is burned as low-energy fuel, which contributes to the waste of renewable resources [1–4].

Lignin is a very interesting and promising macromolecule due to its unique chemical structure (aromatic monomers), high carbon content, and the presence of various functional groups. However, its heterogeneous and recalcitrant structure hinders the applicability of lignin in various industrial sectors [4–6]. To obtain industrial lignin characterized by low polydispersity, homogenous molecular structure, preferred physical properties, chemical reactivity, and low content of impurities, fractionation procedures need to be applied [7–11]. Lignin fractionation procedures are extensively studied in the literature. The most commonly used methods are black liquor ultrafiltration, selective precipitation, and fractionation of lignin with organic solvents [12–15]. The production of lignins with distinct molecular weight distributions and group functionalities is essential for industrial applications. Due to growing global awareness of environmental pollution and the depletion of fossil fuels, current investigations need to be focused on the development of sustainable fractionation methods based on the principles of green chemistry [15–18].

Carbon fibers are engineered materials used in various industrial sectors, such as automotive, aerospace, wind energy, marine industries, and many others [19–21]. Currently, commercialized carbon fibers are mostly manufactured from petroleum-derived polyacrylonitrile (PAN), which is not aligned with sustainable development. Carbon fibers exist in various forms, differing in manufacturing processes, morphology, structure, and applications. Electrospun carbon fibers are a type of carbon that features a non-woven structure with various potential applications, such as reinforced composites, energy storage, sensors, and membrane filtration [22–24]. Lignin, as a large-volume and low-cost industrial by-product, can be considered a potential renewable replacement for PAN in carbon fiber production, including electrospun carbon fibers [9,25–28]. It has a high carbon content of up to 60%, which is similar to PAN, a unique polyaromatic structure that is important to produce different types of carbon fiber for structural and energy-related applications [9,27,29]. Electrospinning of lignin typically requires synthetic polymer additives such as polyethylene oxide (PEO), due to the considerably lower-molecular-weight of lignin compared with common electrospinning polymers like PAN [30,31]. Increasing the polymer concentration in the spinning dope can partially overcome this limitation by enhancing polymer chain entanglement, but the poor solubility of kraft lignin at high concentrations is the limiting factor for this approach [32,33]. Previous studies have demonstrated that solvent fractionation and the use of high-molecular-weight lignin fractions enable electrospinning without polymer additives [26,28,34,35]. However, using undesirable solvents such as methylene chloride and the relatively low fractionation yields are drawbacks [28,34,36]. Therefore, developing a green solvent-based fractionation method with higher yield and efficiency is more desirable for producing refined lignin suitable for electrospun carbon fiber fabrication.

This work focuses on applying a green solvent-based fractionation procedure with high yield to produce electrospun carbon fibers from LignoBoost softwood kraft lignin. Fractionation enabled obtaining lignin with a lower polydispersity and a specific molecular mass, and therefore appropriate physical and chemical properties. This makes it a suitable precursor for producing sustainable carbon fibers without the need for polymer additives typically used to enhance the spinnability of lignin. The use of green solvents and the valorization of lignin as an industrial waste product fit perfectly into the concept of sustainable development.

2. Materials and Methods

2.1. Materials

LignoBoost softwood kraft lignin, produced at RISE LignoDemo (Bäckhammar, Sweden) from pine/spruce black liquor, was used to obtain low- and high-molecular-weight lignin fractions.

2.2. Fractionation of Lignin

Sequential solvent extraction was used to refine lignin, yielding two fractions with distinct molecular weights. Initially, 100 g of lignin was dissolved in ethyl acetate at a solid-to-liquid ratio of 1:10 (w/v) and stirred for 6 h at room temperature. The solution was then filtered, and the recovered solid was air-dried, followed by drying at 80 °C under a vacuum for approximately 12 h. In the second step, the dried solid was extracted with an acetone/water (70:30 v/v) binary solvent at the same solid-to-liquid ratio. This extraction was also performed at room temperature with 6 h of stirring. After filtration, lignin from both filtrates was isolated using a rotary evaporator. The isolated lignins were further dried in a vacuum oven at 80 °C for 12 h. The extraction yields were 18.1% for the first step and 71.8% for the second step. A flowchart summarizing lignin fractionation steps is presented in Figure 1.

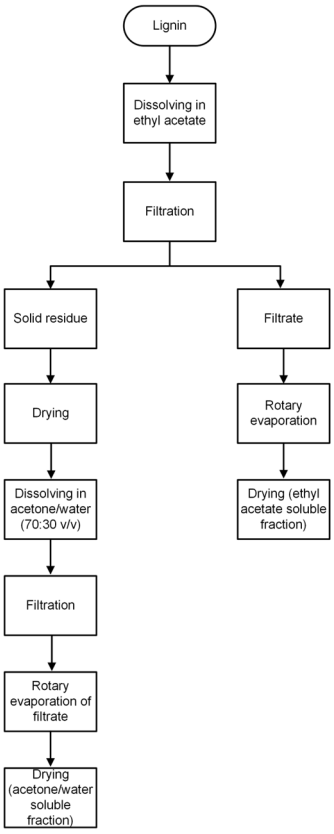


Figure 1. Flowchart illustrating the solvent fractionation of lignin.

2.3. Characterization of Lignins

The carbon, hydrogen, nitrogen, sulfur, and oxygen (CHNS-O) content of the lignin samples was determined using a EuroVector EuroEA3000 elemental analyzer (Pavia, Italy).

The molar mass distribution of the lignin samples was assessed by size-exclusion chromatography (SEC) using a Waters instrument equipped with a Knauer K-2501 UV detector (KNAUER, Berlin, Germany). The separation was performed using two PSS MCX columns (1000 Å and 100,000 Å) connected in series, with a pH 12 aqueous buffer as eluent at 0.5 mL/min. Before analysis, lignin samples were dissolved in NaOH (pH 12), then diluted with the eluent to a suitable concentration. A 100 µL aliquot was injected for each run. Sodium polystyrene sulfonate standards with molecular weights ranging from 250 to 200,000 g/mol were used for calibration.

SEM micrographs of the lignin samples were obtained using a FEI Phenom World scanning electron (FEI Company, Hillsboro, OR, USA) microscope operated at an accelera-

tion voltage of 5 kV. Images were captured at magnifications of 500×, 1000×, and 5000×. To enhance image contrast and minimize charging effects, the samples were sputter-coated with a thin Pd/Au layer using a Polaron SC7640 sputter coater (Quorum Technologies, Lewes, UK) before imaging.

FTIR-ATR spectra of the lignin samples were obtained using a Nicolet 8700 FT-IR spectrometer (Thermo Scientific, Waltham, MA, USA) equipped with a Smart Orbit™ ATR accessory and a DLaTGS detector. Spectra were recorded in the 400–4000 cm^{-1} range with a resolution of 4 cm^{-1}. For each spectrum, the interferograms of 256 scans were averaged. Spectral acquisition and processing were performed using Omnic software (version 8.1), applying baseline correction, normalization, and ATR correction functions. All measurements were conducted in triplicate.

The thermal decomposition of the lignins was analyzed in duplicate using a TA Instruments Q5000 thermogravimetric analyzer (TGA) (TA Instruments, New Castle, DE, USA). Approximately 7 mg of lignin samples were placed in a TGA pan, heated from room temperature to 100 °C, held at this temperature for 10 min to remove any remaining moisture, and then heated to 1000 °C at a rate of 10 °C/min under a nitrogen atmosphere (25 mL/min).

The glass transition temperature (T_g) of the lignin was determined in triplicate on approximately 3 mg samples using a TA Instruments Q2000 differential scanning calorimeter (DSC). (TA Instruments, New Castle, DE, USA). Each sample was heated from 25 °C to 150 °C at a rate of 20 °C/min under nitrogen (50 mL/min), held at 150 °C for 5 min to remove any remaining moisture and erase thermal history, then cooled to 25 °C and reheated to 220 °C at the same rate. The second heating trace was used to calculate T_g and the corresponding heat capacity (ΔCp).

Hydroxyl groups in the lignins were quantified using quantitative ^{31}P NMR spectroscopy on an Avance III 400 MHz NMR(Bruker, Bileric, MA, USA) spectrometer equipped with a broadband PFG 5 mm probe. Lignin samples (30 mg) were dissolved in a dimethylformamide/pyridine (1:1 v/v) mixture and mixed with 100 µL of a solution containing N-hydroxy-5-norbornene-2,3-dicarboxylic acid imide (20 mg/mL) and chromium (III) acetylacetonate (5 mg/mL) as the internal standard and relaxation agent, respectively. The lignins were derivatized with 100 µL of 2-chloro-4,4,5,5-tetramethyl-1,3,2-dioxaphospholane (TMDP) [37,38].

2.4. Electrospinning and Production of Electrospun Carbon Fibers

The electrospinning process was conducted using a 52 wt% solution of the high-molecular-weight lignin fraction (acetone/water soluble) dissolved in dimethylformamide. This solution was loaded into a 5 mL Becton Dickinson plastic syringe (Becton Dickinson, Franklin Lake, NJ, USA) and pushed through a 22-gauge Hamilton syringe needle using a KdScientific pump (Harvard Apparatus, Holliston, MA, USA) at a flow rate of 0.5 mL/h. A Glassman high-voltage power supply was used to generate an electrical field of 17 kV between the needle and collector. The collector was a grounded cylinder (10 cm diameter, 18 cm width) covered with aluminum foil, rotating at 60 rpm. The distance between the needle tip and the collector was 17 cm. Lignin fibers were deposited on the aluminum foil at ambient temperature.

The electrospun lignin fibers were thermostabilized in an MTI Box Furnace (KSL-1200X) (MTI Corporation, Richmond, CA, USA). The temperature was increased from room temperature to 250 °C at a rate of 0.5 °C/min, followed by a 30 min isothermal hold at 250 °C. This process was performed under an airflow of 10 L/min.

The thermostabilized lignin fibers were carbonized in an MTI tube furnace (OTF-1200X) (MTI Corporation, Richmond, CA, USA) under a nitrogen atmosphere (flow rate: 0.3 L/min). The heating profile consisted of two stages: first, from room temperature to 600 °C at a rate

of 3 °C/min, and then from 600 °C to 1000 °C at a rate of 5 °C/min. The fibers were held isothermally for 20 min at the final temperature. The thermostabilization and carbonization yields were 85.3% and 43.2%, respectively.

The morphology of the electrospun carbon fibers was evaluated using a SU3500 Hitachi scanning electron microscope (SEM) (Hitachi High-Technologies Corporation, Tokyo, Japan) at an acceleration voltage of 10 kV at magnifications of 500× and 2000×. The diameter of fibers was measured using ImageJ software (version 1.54g). The SEM micrograph of the green fibers was obtained using the same procedure as for the lignin particles.

3. Results and Discussions

3.1. Properties of Lignin Samples

3.1.1. Elemental Composition

In Table 1, we compare the elemental composition and ash content of the fractionated lignin samples with those of the as-received lignin. The fractionated lignins have lower ash content since inorganics remain mostly insoluble. The LMW-SKL has slightly higher sulfur content compared to both pristine lignin and HMW-SKL. This suggests that the lower-molecular-weight fraction contains a higher proportion of sulfur-rich lignin polymers with a higher solubility in ethyl acetate. The extraction of elemental sulfur using single or mixed organic solvents such as diethyl ether, toluene, and benzene has been previously demonstrated [39]. The findings present a promising approach for reducing inorganic content in lignin, particularly for applications that require low-ash lignin, such as energy storage.

Table 1. Composition of the lignin samples.

Component (%)	SKL	LMW-SKL	HMW-SKL
C	63.6	63.2	63.4
H	5.76	5.25	5.96
N	0.59	0.69	0.66
O [1]	27.4	27.8	27.2
S	1.90	2.83	2.22
Ash [2]	0.75	0.22	0.60

[1] Subtracted from C, H, N, and ash. [2] Ash was determined using the ASTM standard method.

3.1.2. Molecular Weight of Lignins

Table 2 presents the molecular weight characteristics of the lignin samples, revealing significant differences among the fractions obtained through solvent fractionation. The ethyl acetate-soluble fraction exhibits the lowest molecular weight, while the acetone/water-soluble fraction demonstrates the highest. Both fractionated lignin samples show lower polydispersity compared to the as-received lignin, indicating enhanced homogeneity after solvent refining. This improvement is important for high-value lignin applications, as heterogeneity and high polydispersity are considered the main challenges in lignin valorization [40–42].

Table 2. Molar mass and polydispersity of the lignin samples measured by SEC.

Parameter	SKL	LMW-SKL	HMW-SKL
M_w (g/mol) [1]	4350	2060	4550
M_n (g/mol) [2]	1030	810	1220
PD [3]	4.2	2.5	3.7

[1] Weight average molecular weight. [2] Number average molecular weight. [3] Polydispersity index (M_w/M_n).

The relationship between solvent properties and lignin extraction is clear and aligns with the differences in solvent polarities and their impact on lignin solubility. Ethyl acetate, with its lower polarity and hydrogen bonding capacity, results in a lower solubility yield (18.1%) and extraction of low-molecular-weight lignin [40,42,43]. In contrast, the acetone/water binary solvent, with higher polarity and hydrogen bonding capacity, leads to a significantly increased solubility yield (71.8%) and dissolution of high-molecular-weight lignin fractions insoluble in ethyl acetate. The yield of the high-molecular-weight fraction is considerably higher than values previously reported for the fractionation of softwood kraft lignin used in electrospinning without polymer additives, typically around 42% [26,34,35]. This higher yield offers a practical advantage by providing a greater amount of lignin suitable for this specific application.

These findings are consistent with earlier studies on the impact of solvent polarity in lignin fractionation [40–44]. The process effectively refines lignin into two fractions with specific molecular weight ranges and improved homogeneity. This approach opens new possibilities for high-value applications of lignin in various industries, potentially improving the economic feasibility of lignin-based products. The proposed simple solvent refining system offers an additional advantage by using environmentally friendly solvents and eliminating toxic alternatives. This aligns with green chemistry principles, reducing the environmental impact and potential health risks associated with lignin solvent fractionation.

3.1.3. Morphology of Lignin Particles

The morphology of lignin and the obtained lignin fractions was studied using SEM. A slight difference between the original lignin and the obtained fractions can be seen in the shape of particles (Figure 2). Larger agglomerates were observed for the fractionated lignins, likely resulting from interactions between lignin and the extraction solvents. Both fractions exhibited a more defined and uniform particle size compared to the pristine lignin. Additionally, the HMW-SKL particles displayed a rougher surface morphology with more visible pores, whereas the LMW-SKL particles appeared smoother. The particle size of lignin is an important parameter impacting its solubility in solvents or compounding with polymers in thermoplastic, coating, and thermoset applications.

3.1.4. Structural Characterization of Lignin Samples

FTIR spectroscopy is a well-established technique for assessing both the structural features and chemical homogeneity of lignin. The FTIR spectra of LMW-SKL (brown), HMW-SKL (blue), and unfractionated SKL (purple) showed similar profiles in terms of the presence, position, and relative intensity of the major absorption bands, indicating strong structural homogeneity among the lignin samples (Figure 3). The broad band at 3373 cm^{-1} corresponds to –OH stretching vibrations, while the absorption near 2900 cm^{-1} is attributed to C–H stretching in methyl and methylene groups. The peak at 1707 cm^{-1} is assigned to non-conjugated C=O stretching vibrations. Characteristic aromatic skeletal vibrations are clearly visible at 1600–1605 cm^{-1} and 1515 cm^{-1} [45]. The fingerprint region (1500–800 cm^{-1}) shows well-aligned and overlapping peaks, confirming consistent inter-unit linkages and functional group distributions. Overall, the FTIR analysis demonstrates that LMW-SKL, HMW-SKL, and as-received SKL possess nearly identical chemical structures. The fractionation process primarily separates lignin by molecular weight while preserving its core aromatic framework, functional groups, and bonding characteristics.

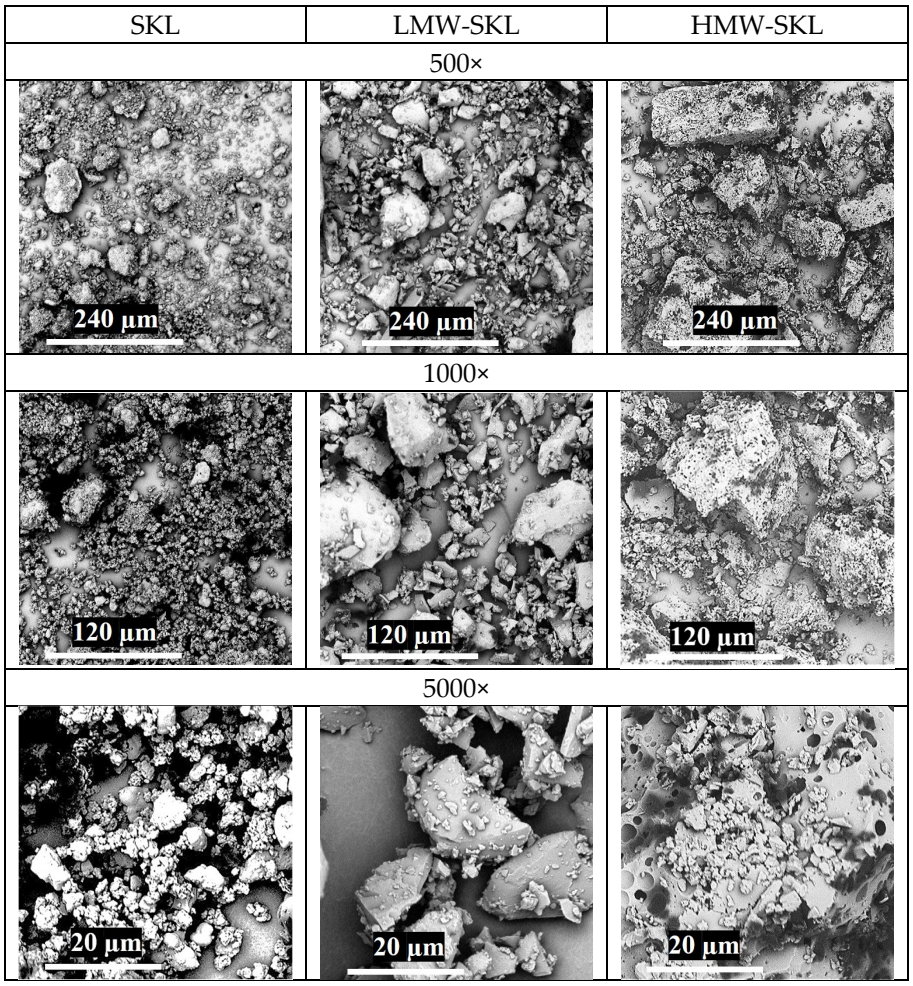


Figure 2. SEM images of the lignin samples.

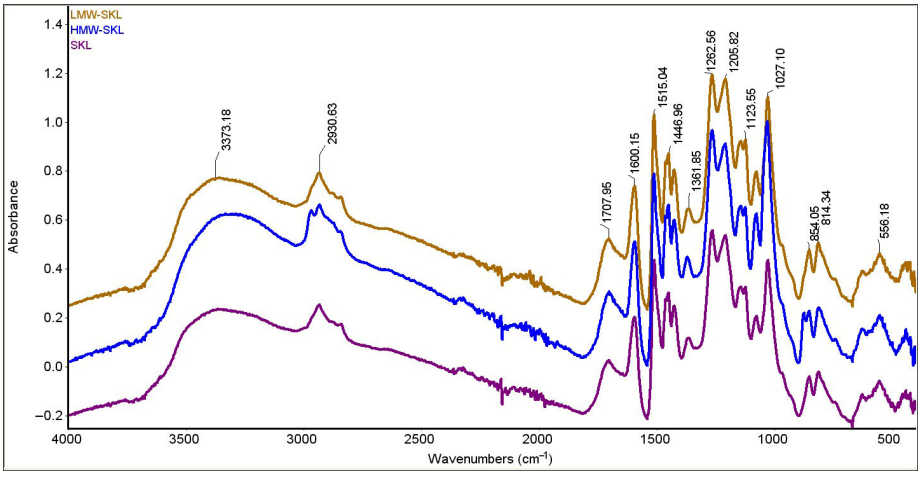


Figure 3. FTIR spectra of the lignin samples.

3.1.5. Thermal Properties of Lignins

Figure 4 presents the DSC thermograms of the lignin samples, with the glass transition temperature (T_g) data summarized in Table 3. The T_g is an important property of lignin, significantly influencing its potential applications in areas such as thermoplastics and carbon fiber production [11,46]. The analysis shows a clear correlation between molecular weight and T_g. The low-molecular-weight lignin (ethyl acetate soluble fraction) has the

lowest T_g (below 100 °C), while the high-molecular-weight lignin (acetone/water soluble fraction) has the highest T_g. This phenomenon can be explained by two primary factors. First, decreasing the molecular weight increases the polymer's free volume, resulting in a lower T_g [43,47]. Second, the high-molecular-weight lignin fraction typically has a higher degree of condensation, which reduces free volume and consequently increases T_g [46,48].

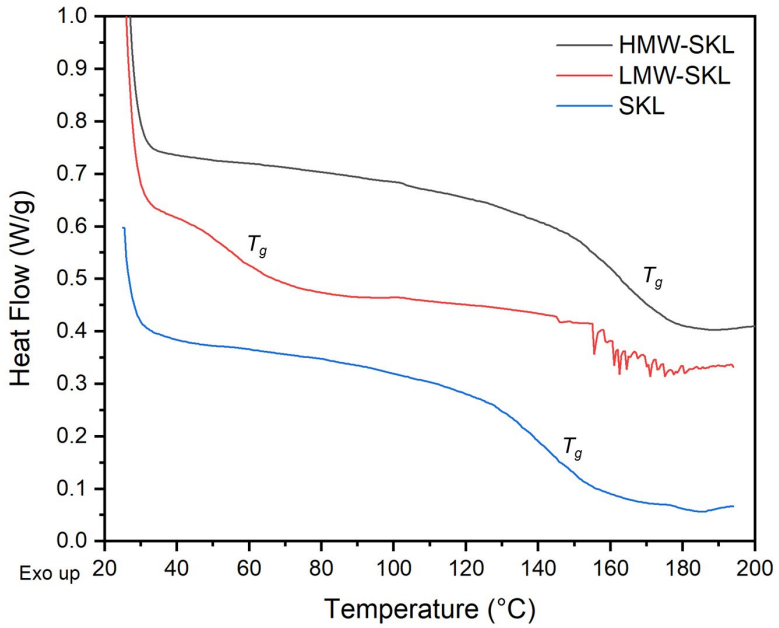


Figure 4. DSC thermograms of the lignin samples.

Table 3. Summary of the DSC results for the lignin samples.

Parameter	SKL	LMW-SKL	HMW-SKL
T_g (°C) [1]	140 (1.15)	56.1 (0.39)	170 (0.34)
Delta Cp (J/g°C)	0.53 (0.01)	0.30 (0.01)	0.50 (0.01)
Transition width (°C)	26.7 (0.58)	15.6 (1.24)	37.5 (1.21)

[1] T_g: Glass transition temperature. Standard deviation is shown in parentheses.

Another important factor influencing T_g is the distribution of hydroxyl groups in the lignin structure. Aliphatic hydroxyl groups, in particular, tend to form strong intermolecular hydrogen bonds that reduce thermal mobility and increase T_g [49,50]. The distribution of hydroxyl groups in the lignin samples and their impact on lignin properties are discussed in detail in the following sections. These findings provide valuable insights into the structure–property relationships of lignin fractions, which can help the selection and modification of lignin for specific applications in materials science and engineering, especially lignin-based polymers.

The thermal decomposition profiles of the lignin samples, presented in Figure 5 and summarized in Table 4, provide important information on their thermal stability. This property is very important, especially in the thermal processing of lignin, impacting processing temperatures and indicating volatile formation at specific temperatures. The TGA profiles and extracted data, including the temperature at 5% weight loss ($T_{5wt\%}$), temperature at 50% weight loss ($T_{50wt\%}$), and temperature of maximum decomposition rate (T_{max}), are important indicators for comparing the thermal stability of lignin samples.

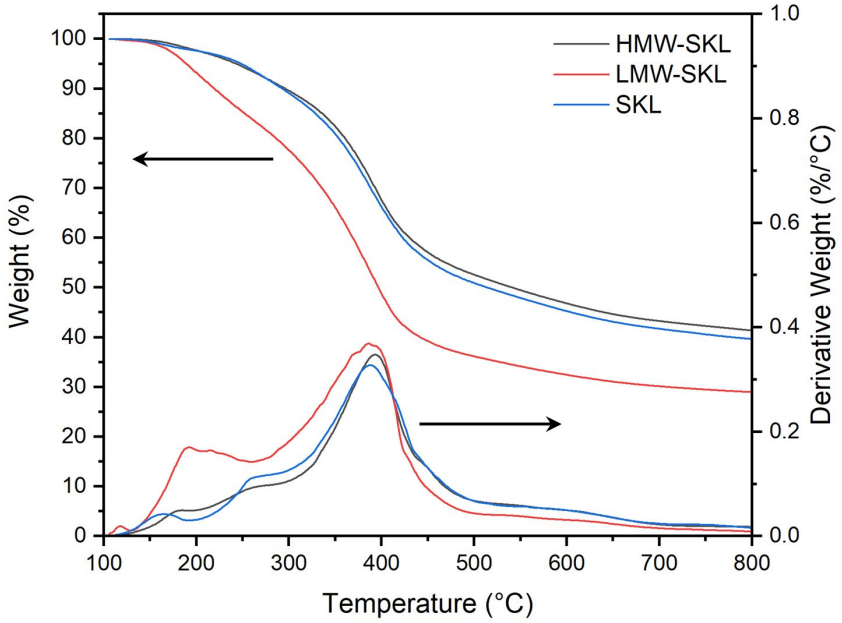


Figure 5. Thermal decomposition profile of the lignin samples.

Table 4. Summary of key data related to the thermal decomposition of the lignin samples.

Parameter	SKL	LMW-SKL	HMW-SKL
$T_{5wt\%}$ (°C) [1]	248	189	244
$T_{50wt\%}$ (°C) [2]	514	396	540
T_{max} (°C) [3]	388	386	394
Δ Mass at T_{max} (%)	70.1	53.9	69.9
Residue at 1000 °C (%)	37.7	28.3	40.0

[1] $T_{5wt\%}$: starting thermal decomposition temperature (the temperature at 5% weight loss). [2] $T_{50wt\%}$: temperature at 50% weight loss. [3] T_{max}: temperature of maximum decomposition rate (taken from the derivative thermogravimetric analysis (DTG)).

Analysis of the data reveals a clear correlation between molecular weight and thermal stability. The LMW-SKL exhibits the lowest thermal stability and residual char content. In contrast, the HMW-SKL demonstrates the highest thermal stability and residual char, indicative of its higher fixed carbon content. In addition, the LMW-SKL shows significantly lower thermal stability at temperatures below 300 °C compared to both HMW-SKL and the as-received lignin (SKL).

The observed differences in thermal stability are primarily attributed to variations in molecular weight. It has been shown that higher-molecular-weight lignin fractions have a higher thermal stability compared to the lower-molecular-weight fractions [43,47,48]. This observation is linked to the more condensed structure of high-molecular-weight lignin, which enhances both thermal stability and char yield [43,47,48]. Additionally, the higher concentration of functional groups in lower-molecular-weight lignins contributes to their reduced thermal stability [43,47,50].

Based on the thermal analysis results, the fractionation process has successfully produced two lignin fractions with distinct thermal properties, particularly in terms of thermal mobility/fusibility and stability. These distinct characteristics can open up a range of potential applications for each fraction. The high-molecular-weight lignin, with its higher thermal stability and char yield, is well-suited for applications such as electrospinning and as a carbon precursor. It has been shown that a high-molecular-weight lignin fraction, characterized by a higher char yield and T_g, leads to increased carbon yield and enables rapid thermostabilization without fiber fusion [34]. On the other hand, the low-molecular-weight

lignin, with its lower T_g and higher fusibility, can potentially have better melt processability, making it more suitable for applications such as thermoplastics, binders, and melt-spinning processes.

3.1.6. Quantifying Hydroxyl Group Distribution in Lignins

Figure 6 presents the ^{31}P NMR spectra, while Table 5 compares the number and distribution of hydroxyl groups (OH) in different lignin samples. The distribution and quantity of hydroxyl groups play an important role in determining lignin functionality and thermal properties, including glass transition temperature and thermal stability [51,52].

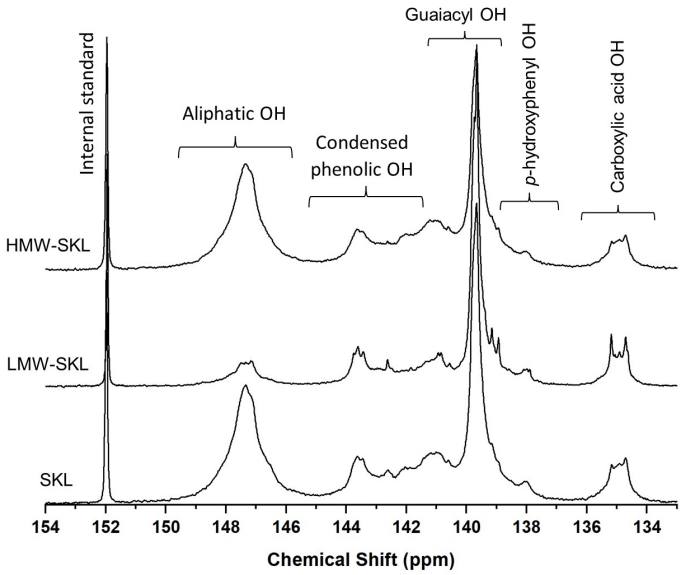


Figure 6. Quantitative ^{31}P NMR spectra and signal assignment of the lignin samples.

Table 5. Results of quantitative analysis of hydroxyl groups of lignins using ^{31}P NMR spectroscopy (mmol/g).

Sample	Carboxylic Acid OH	Phenolic OH			Total Phenolic OH	Aliphatic OH
		p-Hydroxyphenyl	Condensed Phenolic	Guaiacyl		
SKL	0.55	0.17	1.70	2.25	4.12	2.14
LMW-SKL	0.69	0.21	1.64	2.88	4.73	0.70
HMW-SKL	0.43	0.20	1.66	2.04	3.90	2.14

Analysis of the data reveals significant differences in OH group distribution among the lignin fractions. The LMW-SKL has a significantly lower number of aliphatic OH groups compared to both the HMW-SKL and the as-received lignin. Additionally, LMW-SKL has a higher number of phenolic OH groups, particularly guaiacyl OH, and carboxylic acid OH groups. This distribution pattern can be attributed to the selective solubility of ethyl acetate, which, due to its low polarity and limited number of free OH groups, selectively dissolves the smaller lignin fraction with lower molecular weight and fewer aliphatic OH groups [48].

The observed OH group distribution correlates strongly with the thermal properties of the lignin fractions. The higher T_g of HMW-SKL, as demonstrated in the DSC results, can be partially due to its greater number of aliphatic OH groups. These groups form intermolecular hydrogen bonds, reducing molecular motion and increasing T_g [51,52]. In contrast, the phenolic OH groups, which are higher in LMW-SKL, tend to form intramolecular hydrogen bonds, limiting intermolecular interactions and resulting in a lower T_g [52].

The results of the ^{31}PNMR analysis are consistent with previous findings on the impact of solvent fractionation on lignin OH group distribution [44,48], confirming the reliability of the method in producing lignin fractions with predictable and tunable properties. The distinct OH group profiles impact specific functionalities and properties of each fraction, broadening the potential application of lignin. For example, variations in phenolic OH content may affect nucleation and condensation behavior during nanoprecipitation, influencing lignin nanoparticle formation [53]. Moreover, the higher aliphatic OH content and corresponding elevated T_g in the HMW-SKL fraction are important factors for rapid stabilization and carbonization during lignin-based carbon fiber production [35,46].

3.2. Electrospinning and Electrospun Carbon Fibers

We used the high-molecular-weight lignin fraction for electrospinning and producing lignin-based electrospun carbon fibers. Previous studies have shown that the high-molecular-weight lignin is the most suited lignin fraction for electrospinning of lignin without any polymer additives [34,35]. The relatively lower molecular weight of lignin compared to the synthetic polymers prevents the formation of fibers during electrospinning, and a polymer additive such as PEO with a higher molecular weight is needed to facilitate the electrospinning of lignin [30,54]. Generally, lower molecular weight results in the formation of beads and droplets [55]. In this situation, a higher concentration of polymer in the dope solution can increase the polymer chain entanglement, help to overcome the surface tension of the solution, and stretch the liquid jet to prevent the formation of beads and droplets [55–57]. However, there are limitations such as the maximum capacity of solubility, blockage of flow in the needle, drying of the solution at the needle tip, and increasing the fiber diameter in high-concentration dope solutions [55,58]. Therefore, the best approach is to use a high-molecular-weight lignin fraction with good solubility for producing electrospun fibers without any synthetic polymer additive. Removing the insoluble residual using the solvent fractionation is an important factor that helps to have a perfectly dissolved fractionated lignin at a high concentration for producing spinning dope. Additionally, the polymer additive, particularly PEO, has a negative impact on stabilization and carbonization by increasing the fusibility of lignin and the need for a slow rate of stabilization to prevent fiber fusion during the thermal conversion step [59]. Previously, a solvent fractionation method showed the possibility of producing pure lignin electrospun fibers and fast conversion of the resulting fibers from a high-molecular-weight lignin fraction. However, the reported solvent extraction was based on a high-molecular-weight lignin from a methanol/methylene chloride binary solvent and a relatively low fractionation yield [34,35]. Methylene chloride has been listed as an undesirable solvent [60]. Here, we demonstrate the solvent fraction of lignin using green and preferred solvents, with a high fractionation yield, and using the high-molecular-weight fraction as a precursor for pure lignin electrospinning and producing electrospun lignin-based carbon fibers. The electrospinning resulted in the continued formation of electrospun fibers and resulted in carbon fibers showing a uniform electrospun carbon fiber mat with an average fiber diameter of 559 $\pm$ 216 nm (Figure 7). The diameter of the carbonized fibers is in the range of diameters previously reported for lignin-based electrospun carbon fibers from refined kraft lignin [26,28,35]. These values are even smaller than some of the values reported on the electrospinning of kraft lignin with polymer additives [30,33]. Successful electrospinning was achieved without polymer additives, producing green fibers with relatively uniform morphology. These fibers were successfully converted to carbonized fibers without fusing, maintaining relatively uniform morphology and diameters comparable to previous reports [34,35], thereby demonstrating the advantage of high-molecular-weight lignin fractions for producing electrospun carbon fiber.

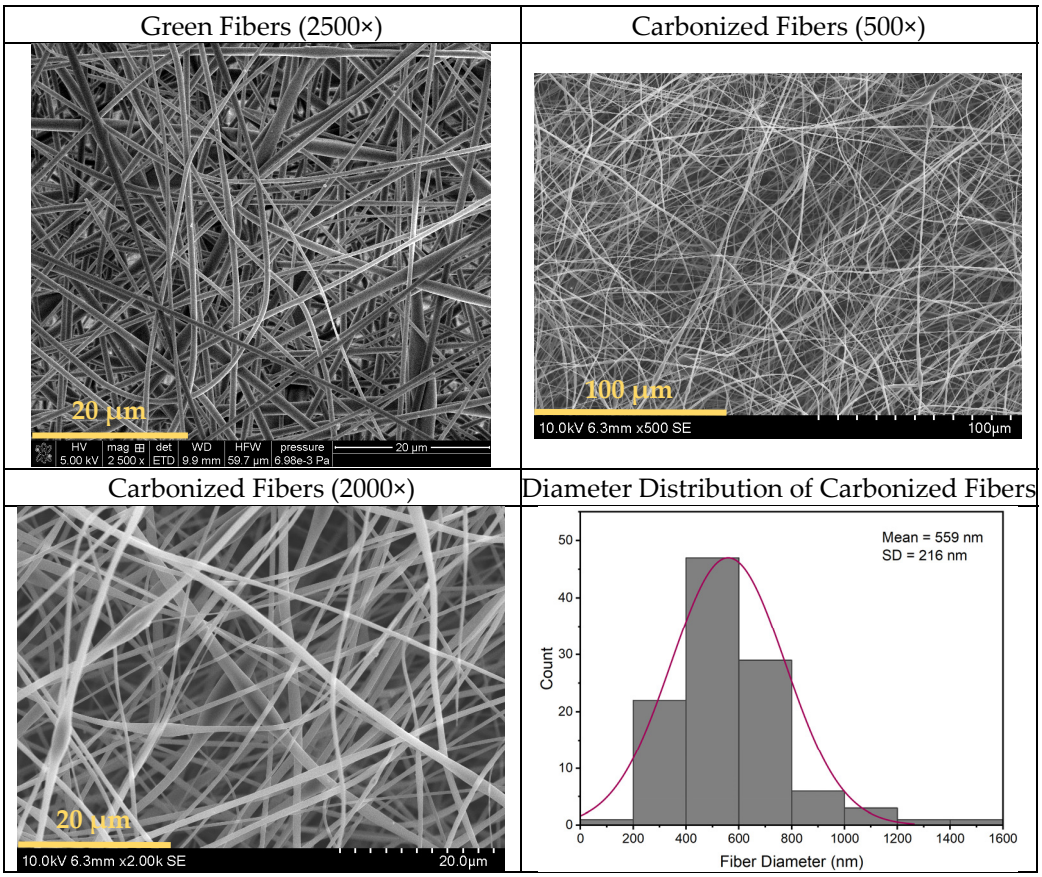


Figure 7. SEM images and diameter distribution of electrospun fibers.

This study advances the lignin valorization field by demonstrating the effectiveness of a green solvent-based fractionation method for isolating high-molecular-weight lignin suitable for electrospinning. The findings not only contribute to the ongoing efforts in lignin valorization but also align with broader sustainability objectives in materials science. By establishing the feasibility of green solvents for lignin fractionation in high-value applications, this work promotes the development of more sustainable and environmentally responsible pathways for carbon fiber production and related technologies.

4. Conclusions

The presented solvent fractionation process effectively refined lignin into fractions with specific molecular weight ranges, thermal properties, and improved homogeneity. The use of environmentally friendly solvents while avoiding toxic alternatives aligns with green chemistry principles and reduces the negative environmental impact. A clear correlation was observed between lignin molecular weight and T_g, as well as the thermal properties. The high-molecular-weight lignin fraction enabled the production of lignin-based electrospun carbon fibers without any polymer additives. The high fractionation yield, elevated glass transition temperature, high dope concentration, and high char yield collectively enable efficient production of lignin-based electrospun carbon fibers and accelerate the conversion process. These findings not only demonstrate the structure–property relationships in fractionated lignin but also offer valuable insights for selecting suitable lignin fractions for specific thermal processing applications. The ability to tailor lignin properties through fractionation can be considered a significant step forward in lignin valorization, expanding its potential for various high-value industrial applications.

Author Contributions: Conceptualization, O.H.; methodology, M.G.-C. and O.H.; validation, M.G.-C. and O.H.; formal analysis, M.G.-C. and O.H.; investigation, M.G.-C. and O.H.; resources, M.G.-C. and O.H.; data curation, M.G.-C. and O.H.; writing—original draft, M.G.-C. and O.H.; writing—review and editing, M.G.-C. and O.H.; visualization, M.G.-C. and O.H.; supervision, O.H.; project administration, M.G.-C. and O.H. All authors have read and agreed to the published version of the manuscript.

Funding: This research received no external funding.

Data Availability Statement: All data supporting the findings of this study are included in the article. Further inquiries can be directed to the corresponding authors.

Acknowledgments: This publication is based on collaboration within the COST Action Waste Biorefinery Technologies for Accelerating Sustainable Energy Processes (WIRE), CA20127, supported by COST (European Cooperation in Science and Technology); www.cost.eu (accessed on 1 December 2025).

Conflicts of Interest: The authors declare no conflicts of interest.

Abbreviations

The following abbreviations are used in this manuscript:

SKL	Softwood kraft lignin
LMW-SKL	Low-molecular-weight softwood kraft lignin
HMW-SKL	High-molecular-weight softwood kraft lignin
T_g	Glass transition temperature

References

1. Bajwa, D.S.; Pourhashem, G.; Ullah, A.H.; Bajwa, S.G. A Concise Review of Current Lignin Production, Applications, Products and Their Environmental Impact. *Ind. Crops Prod.* **2019**, *139*, 111526. [CrossRef]
2. Argyropoulos, D.D.S.; Crestini, C.; Dahlstrand, C.; Furusjö, E.; Gioia, C.; Jedvert, K.; Henriksson, G.; Hulteberg, C.; Lawoko, M.; Pierrou, C.; et al. Kraft Lignin: A Valuable, Sustainable Resource, Opportunities and Challenges. *ChemSusChem* **2023**, *16*, e202300492. [CrossRef]
3. Dessbesell, L.; Paleologou, M.; Leitch, M.; Pulkki, R.; Xu, C. Global Lignin Supply Overview and Kraft Lignin Potential as an Alternative for Petroleum-Based Polymers. *Renew. Sustain. Energy Rev.* **2020**, *123*, 109768. [CrossRef]
4. Sun, R.C. Lignin Source and Structural Characterization. *ChemSusChem* **2020**, *13*, 4385–4393. [CrossRef]
5. Sethupathy, S.; Murillo Morales, G.; Gao, L.; Wang, H.; Yang, B.; Jiang, J.; Sun, J.; Zhu, D. Lignin Valorization: Status, Challenges and Opportunities. *Bioresour. Technol.* **2022**, *347*, 126696. [CrossRef]
6. Yoo, C.G.; Ragauskas, A.J. Opportunities and Challenges of Lignin Utilization. In *Lignin Utilization Strategies: From Processing to Applications*; ACS Symposium Series; American Chemical Society: Washington, DC, USA, 2021; Volume 1377, pp. 1–12. ISBN 9780841298460.
7. Xu, J.; Li, C.; Dai, L.; Xu, C.; Zhong, Y.; Yu, F.; Si, C. Biomass Fractionation and Lignin Fractionation towards Lignin Valorization. *ChemSusChem* **2020**, *13*, 4284–4295. [CrossRef]
8. Jin, J.; Ding, J.; Klett, A.; Thies, M.C.; Ogale, A.A. Carbon Fibers Derived from Fractionated–Solvated Lignin Precursors for Enhanced Mechanical Performance. *ACS Sustain. Chem. Eng.* **2018**, *6*, 14135–14142. [CrossRef]
9. Wang, S.; Bai, J.; Innocent, M.T.; Wang, Q.; Xiang, H.; Tang, J.; Zhu, M. Lignin-Based Carbon Fibers: Formation, Modification and Potential Applications. *Green Energy Environ.* **2022**, *7*, 578–605. [CrossRef]
10. Beaudoin, D.; Langis-Barsetti, S.; Gagné, A.; Palus, E.; Inwood, J.; Konduri, M.K.R. Aqueous Ethanol Fractionation of Softwood and Hardwood Kraft Lignins: Impact on Purity and Properties. *J. Wood Chem. Technol.* **2024**, *44*, 133–144. [CrossRef]
11. Wang, C.; Kelley, S.S.; Venditti, R.A. Lignin-Based Thermoplastic Materials. *ChemSusChem* **2016**, *9*, 770–783. [CrossRef]
12. Sadeghifar, H.; Ragauskas, A. Perspective on Technical Lignin Fractionation. *ACS Sustain. Chem. Eng.* **2020**, *8*, 8086–8101. [CrossRef]
13. Gigli, M.; Crestini, C. Fractionation of Industrial Lignins: Opportunities and Challenges. *Green Chem.* **2020**, *22*, 4722–4746. [CrossRef]
14. Chatterjee, S.; Saito, T. Solvent Fractionation of Lignin. In *Polymer Precursor-Derived Carbon*; American Chemical Society: Washington, DC, USA, 2014; Volume 1173, pp. 153–168. ISBN 0-8412-2966-X.
15. Rodrigues, J.S.; Lima, V.; Araújo, L.C.P.; Botaro, V.R. Lignin Fractionation Methods: Can Lignin Fractions Be Separated in a True Industrial Process? *Ind. Eng. Chem. Res.* **2021**, *60*, 10863–10881. [CrossRef]

16. Ragauskas, A.J.; Beckham, G.T.; Biddy, M.J.; Chandra, R.; Chen, F.; Davis, M.F.; Davison, B.H.; Dixon, R.A.; Gilna, P.; Keller, M.; et al. Lignin Valorization: Improving Lignin Processing in the Biorefinery. *Science* **2014**, *344*, 1246843. [CrossRef]
17. Ajao, O.; Jeaidi, J.; Benali, M.; Abdelaziz, O.Y.; Hulteberg, C.P. Green Solvents-Based Fractionation Process for Kraft Lignin with Controlled Dispersity and Molecular Weight. *Bioresour. Technol.* **2019**, *291*, 121799. [CrossRef] [PubMed]
18. Vishtal, A.G.; Kraslawski, A. Challenges in Industrial Applications of Technical Lignins. *Bioresources* **2011**, *6*, 3547–3568. [CrossRef]
19. Chand, S. Review Carbon Fibers for Composites. *J. Mater. Sci.* **2000**, *35*, 1303–1313. [CrossRef]
20. Frank, E.; Steudle, L.M.; Ingildeev, D.; Spörl, J.M.; Buchmeiser, M.R. Carbon Fibers: Precursor Systems, Processing, Structure, and Properties. *Angew. Chem. Int. Ed.* **2014**, *53*, 5262–5298. [CrossRef] [PubMed]
21. Hiremath, N.; Mays, J.; Bhat, G. Recent Developments in Carbon Fibers and Carbon Nanotube-Based Fibers: A Review. *Polym. Rev.* **2017**, *57*, 339–368. [CrossRef]
22. Fang, W.; Yang, S.; Wang, X.-L.; Yuan, T.-Q.; Sun, R.-C. Manufacture and Application of Lignin-Based Carbon Fibers (LCFs) and Lignin-Based Carbon Nanofibers (LCNFs). *Green Chem.* **2017**, *19*, 1794–1827. [CrossRef]
23. Mao, X.; Hatton, T.A.; Rutledge, G.C. A Review of Electrospun Carbon Fibers as Electrode Materials for Energy Storage. *Curr. Org. Chem.* **2013**, *17*, 1390–1401. [CrossRef]
24. Zhang, L.; Aboagye, A.; Kelkar, A.; Lai, C.; Fong, H. A Review: Carbon Nanofibers from Electrospun Polyacrylonitrile and Their Applications. *J. Mater. Sci.* **2014**, *49*, 463–480. [CrossRef]
25. Ruiz-Rosas, R.; Bedia, J.; Lallave, M.; Loscertales, I.G.; Barrero, A.; Rodríguez-Mirasol, J.; Cordero, T. The Production of Submicron Diameter Carbon Fibers by the Electrospinning of Lignin. *Carbon* **2010**, *48*, 696–705. [CrossRef]
26. Peuvot, K.; Hosseinaei, O.; Tomani, P.; Zenkert, D.; Lindbergh, G. Lignin Based Electrospun Carbon Fiber Anode for Sodium Ion Batteries. *J. Electrochem. Soc.* **2019**, *166*, A1984–A1990. [CrossRef]
27. Baker, D.A.; Rials, T.G. Recent Advances in Low-Cost Carbon Fiber Manufacture from Lignin. *J. Appl. Polym. Sci.* **2013**, *130*, 713–728. [CrossRef]
28. Schlee, P.; Hosseinaei, O.; Baker, D.; Landmér, A.; Tomani, P.; Mostazo-López, M.J.; Cazorla-Amorós, D.; Herou, S.; Titirici, M.-M.M. From Waste to Wealth: From Kraft Lignin to Free-Standing Supercapacitors. *Carbon* **2019**, *145*, 470–480. [CrossRef]
29. Sun, S.-C.; Xu, Y.; Wen, J.-L.; Yuan, T.-Q.; Sun, R.-C. Recent Advances in Lignin-Based Carbon Fibers (LCFs): Precursors, Fabrications, Properties, and Applications. *Green Chem.* **2022**, *24*, 5709–5738. [CrossRef]
30. Dallmeyer, I.; Ko, F.; Kadla, J.F. Electrospinning of Technical Lignins for the Production of Fibrous Networks. *J. Wood Chem. Technol.* **2010**, *30*, 315–329. [CrossRef]
31. Wang, S.-X.; Yang, L.; Stubbs, L.P.; Li, X.; He, C. Lignin-Derived Fused Electrospun Carbon Fibrous Mats as High Performance Anode Materials for Lithium Ion Batteries. *ACS Appl. Mater. Interfaces* **2013**, *5*, 12275–12282. [CrossRef]
32. Passoni, V.; Scarica, C.; Levi, M.; Turri, S.; Griffini, G. Fractionation of Industrial Softwood Kraft Lignin: Solvent Selection as a Tool for Tailored Material Properties. *ACS Sustain. Chem. Eng.* **2016**, *4*, 2232–2242. [CrossRef]
33. Dallmeyer, I.; Lin, L.T.; Li, Y.; Ko, F.; Kadla, J.F. Preparation and Characterization of Interconnected, Kraft Lignin-Based Carbon Fibrous Materials by Electrospinning. *Macromol. Mater. Eng.* **2014**, *299*, 540–551. [CrossRef]
34. Baker, D.A.; Hosseinaei, O. High Glass Transition Lignins and Lignin Derivatives for the Manufacture of Carbon and Graphite Fibers. U.S. Patent 20140271443 A1, 18 September 2014. Available online: https://patents.google.com/patent/US20140271443A1/en (accessed on 1 December 2025).
35. Schlee, P.; Hosseinaei, O.; O' Keefe, C.A.; Mostazo-López, M.J.; Cazorla-Amorós, D.; Herou, S.; Tomani, P.; Grey, C.P.; Titirici, M.-M. Hardwood versus Softwood Kraft Lignin—Precursor-Product Relationships in the Manufacture of Porous Carbon Nanofibers for Supercapacitors. *J. Mater. Chem. A* **2020**, *8*, 23543–23554. [CrossRef]
36. Mikeš, P.; Baker, D.A.; Uhlin, A.; Lukáš, D.; Kuželová-Košťáková, E.; Vidrich, A.; Valtera, J.; Kopřivová, B.; Asatiani, N.; Salmén, L.; et al. The Mass Production of Lignin Fibres by Means of Needleless Electrospinning. *J. Polym. Environ.* **2021**, *29*, 2164–2173. [CrossRef]
37. Granata, A.; Argyropoulos, D.S. 2-Chloro-4,4,5,5-Tetramethyl-1,3,2-Dioxaphospholane, a Reagent for the Accurate Determination of the Uncondensed and Condensed Phenolic Moieties in Lignins. *J. Agric. Food Chem.* **1995**, *43*, 1538–1544. [CrossRef]
38. Rönnols, J.; Schweinebarth, H.; Jacobs, A.; Stevanic Srndovic, J.; Olsson, A.-M.; Reimann, A.; Aldaeus, F. Structural Changes in Softwood Kraft Lignin during Nonoxidative Thermal Treatment. *Nord. Pulp Paper Res. J.* **2015**, *30*, 550–561. [CrossRef]
39. Evdokimov, A.N.; Kurzin, A.V.; Fedorova, O.V.; Lukanin, P.V.; Kazakov, V.G.; Trifonova, A.D. Desulfurization of Kraft Lignin. *Wood Sci. Technol.* **2018**, *52*, 1165–1174. [CrossRef]
40. Ponnuchamy, V.; Gordobil, O.; Diaz, R.H.; Sandak, A.; Sandak, J. Fractionation of Lignin Using Organic Solvents: A Combined Experimental and Theoretical Study. *Int. J. Biol. Macromol.* **2021**, *168*, 792–805. [CrossRef]
41. Pang, T.; Wang, G.; Sun, H.; Sui, W.; Si, C. Lignin Fractionation: Effective Strategy to Reduce Molecule Weight Dependent Heterogeneity for Upgraded Lignin Valorization. *Ind. Crops Prod.* **2021**, *165*, 113442. [CrossRef]

42. Liu, R.; Smeds, A.; Wang, L.; Pranovich, A.; Hemming, J.; Willför, S.; Zhang, H.; Xu, C. Fractionation of Lignin with Decreased Heterogeneity: Based on a Detailed Characteristics Study of Sequentially Extracted Softwood Kraft Lignin. *ACS Sustain. Chem. Eng.* **2021**, *9*, 13862–13873. [CrossRef]
43. Park, S.Y.; Kim, J.-Y.; Youn, H.J.; Choi, J.W. Fractionation of Lignin Macromolecules by Sequential Organic Solvents Systems and Their Characterization for Further Valuable Applications. *Int. J. Biol. Macromol.* **2018**, *106*, 793–802. [CrossRef]
44. Boeriu, C.G.; Fiţigău, F.I.; Gosselink, R.J.A.; Frissen, A.E.; Stoutjesdijk, J.; Peter, F. Fractionation of Five Technical Lignins by Selective Extraction in Green Solvents and Characterisation of Isolated Fractions. *Ind. Crops Prod.* **2014**, *62*, 481–490. [CrossRef]
45. Boeriu, C.G.; Bravo, D.; Gosselink, R.J.A.; van Dam, J.E.G. Characterisation of Structure-Dependent Functional Properties of Lignin with Infrared Spectroscopy. *Ind. Crops Prod.* **2004**, *20*, 205–218. [CrossRef]
46. Hosseinaei, O.; Harper, D.P.; Bozell, J.J.; Rials, T.G. Role of Physicochemical Structure of Organosolv Hardwood and Herbaceous Lignins on Carbon Fiber Performance. *ACS Sustain. Chem. Eng.* **2016**, *4*, 5785–5798. [CrossRef]
47. Yoshida, H.; Morck, R.; Kringstad, K.P.; Hatakeyama, H. Fractionation of Kraft Lignin by Successive Extraction with Organic Solvents. II. Thermal Properties of Kraft Lignin Fractions. *Holzforschung* **1987**, *41*, 171–176. [CrossRef]
48. Izaguirre, N.; Robles, E.; Llano-Ponte, R.; Labidi, J.; Erdocia, X. Fine-Tune of Lignin Properties by Its Fractionation with a Sequential Organic Solvent Extraction. *Ind. Crops Prod.* **2022**, *175*, 114251. [CrossRef]
49. Kubo, S.; Kadla, J.F. Hydrogen Bonding in Lignin: A Fourier Transform Infrared Model Compound Study. *Biomacromolecules* **2005**, *6*, 2815–2821. [CrossRef] [PubMed]
50. Jakab, E.; Faix, O.; Till, F. Thermal Decomposition of Milled Wood Lignins Studied by Thermogravimetry/Mass Spectrometry. *J. Anal. Appl. Pyrolysis* **1997**, *40–41*, 171–186. [CrossRef]
51. Baumberger, S.; Dole, P.; Lapierre, C. Using Transgenic Poplars to Elucidate the Relationship between the Structure and the Thermal Properties of Lignins. *J. Agric. Food Chem.* **2002**, *50*, 2450–2453. [CrossRef]
52. Kubo, S.; Kadla, J.F. Poly(Ethylene Oxide)/Organosolv Lignin Blends: Relationship between Thermal Properties, Chemical Structure, and Blend Behavior. *Macromolecules* **2004**, *37*, 6904–6911. [CrossRef]
53. Lee, J.H.; Kim, T.M.; Choi, I.-G.; Choi, J.W. Phenolic Hydroxyl Groups in the Lignin Polymer Affect the Formation of Lignin Nanoparticles. *Nanomaterials* **2021**, *11*, 1790. [CrossRef]
54. Poursorkhabi, V.; Mohanty, A.K.; Misra, M. Electrospinning of Aqueous Lignin/Poly(Ethylene Oxide) Complexes. *J. Appl. Polym. Sci.* **2015**, *132*, 41260. [CrossRef]
55. Koski, A.; Yim, K.; Shivkumar, S. Effect of Molecular Weight on Fibrous PVA Produced by Electrospinning. *Mater. Lett.* **2004**, *58*, 493–497. [CrossRef]
56. Reneker, D.H.; Yarin, A.L. Electrospinning Jets and Polymer Nanofibers. *Polymer* **2008**, *49*, 2387–2425. [CrossRef]
57. Li, D.; Xia, Y. Electrospinning of Nanofibers: Reinventing the Wheel? *Adv. Mater.* **2004**, *16*, 1151–1170. [CrossRef]
58. Deitzel, J.M.; Kleinmeyer, J.; Harris, D.; Beck Tan, N.C. The Effect of Processing Variables on the Morphology of Electrospun Nanofibers and Textiles. *Polymer* **2001**, *42*, 261–272. [CrossRef]
59. Kadla, J.F.; Kubo, S.; Venditti, R.A.; Gilbert, R.D.; Compere, A.L.; Griffith, W. Lignin-Based Carbon Fibers for Composite Fiber Applications. *Carbon* **2002**, *40*, 2913–2920. [CrossRef]
60. Alfonsi, K.; Colberg, J.; Dunn, P.J.; Fevig, T.; Jennings, S.; Johnson, T.A.; Kleine, H.P.; Knight, C.; Nagy, M.A.; Perry, D.A.; et al. Green Chemistry Tools to Influence a Medicinal Chemistry and Research Chemistry Based Organisation. *Green Chem.* **2008**, *10*, 31–36. [CrossRef]

Disclaimer/Publisher's Note: The statements, opinions and data contained in all publications are solely those of the individual author(s) and contributor(s) and not of MDPI and/or the editor(s). MDPI and/or the editor(s) disclaim responsibility for any injury to people or property resulting from any ideas, methods, instructions or products referred to in the content.